Experimental investigation on the distribution of along-wind loading on a high-rise building with rectangular section

Jiadong Zeng[1], Mingshui Li[2] and Shaopeng Li[3]

[1), 2), 3)] *Research Center for Wind Engineering, Southwest Jiaotong University, Chengdu, Sichuan 610031, China*
[1)] *zjd_rcwe@126.com*

ABSTRACT

The distribution of the aerodynamic loads, pressures and drag forces, on a high-rise building with rectangular cross configuration (2:1) are investigated by wind tunnel testing. The synchronically surface pressures on the rigid model were measured in simulated atmospheric boundary layer flow. The unsteady drag force was calculated by numerical integral of surface pressure. The results show that the pressures and drag forces were more correlated than the incident gusty wind, which indicated the invalidity of traditional coherence model, the collapse factor in the exponential coherence model was not constant. An extended empirical coherence model of along-wind loading was proposed by taking the effects of B (width of the structure) and L_u (scale of the turbulence) into consideration.

1. INTRODUCTION

With the modern high-rise building toward super-high and flexible, wind loading has become one of dominant loads in structural design. The method of synchronous manometric test is usually adopted to obtain the time history of wind pressures on the surface of the rigidity model. The statistical characteristics of wind pressures, the mean values, the root-mean-square (RSM), the spectra and spatial correlations ect., can be calculated, and the overall static and dynamic wind loads can be obtained by integrating the surface pressures of the building. Regarding to this issue, many researchers have made meaningful studies. Kareem (1990) presented measurements and analyses of space-time structure of random pressure fields and associated area-averaged loads acting on prismatic building models in simulated atmospheric flows. Vickery (1966) investigated the fluctuating lift and drag on a long square cylinder, and his measurements also included the correlation of lift along the cylinder and the distribution of fluctuating pressure on a cross-section. Huot et al. (1986) studied the mean and fluctuating pressure field that develop on the surface of a square cylinder (side D) immersed in homogeneous flows with different intensities ($u'/\overline{U}_\infty$), ratios of turbulence scales to cylinder scale. Based on the experimental investigation on rectangular cylinders with various side ratios, Liang et al. (2002) proposed a series of

---

[1), 3)] PhD student
[2)] Professor

empirical formulas, including torque spectra, RMS torque coefficients and Strouhal number, as well as coherence functions of torque. Gu (2006) measured the mean and fluctuating wind pressure distributions with 10 typical super-tall building models, the mean and RMS coefficients of the drag, lift and torsion moment on the measuring layers were obtained from the wind pressures.

In this paper, the surface pressures on rectangular section rigidity model (side ratio 2: 1) were measured synchronically in passive simulated atmospheric boundary layer flow, the possible effects of height of the building, wind speeds and integral length scales on the spectra of dynamic loads and spatial coherences are discussed. Then, based on the measured results, a general coherence model of unsteady wind loads on high-rise building, by taking the effect of width of the building and the integral length scale of turbulence into consideration, was proposed and the error margin of the traditional gusty wind coherence model was also estimated.

2. WIND TUNNEL TESTS

The experiments in this study were carried out in the XNJD-3 industrial wind tunnel at Southwest Jiaotong University which is the world's largest boundary layer wind tunnel so far. The wind tunnel has a working section of 22.5m (width) $\times$ 4.5m (height) $\times$ 36m (length) and a wind speed range of 1.0 ~ 16.5m/s. The model is 2.3m in height, and the dimension of rectangular cross-section is 20 cm$\times$10cm (B/D=2:1). The model is fixed to the bottom of the test section as shown in Fig. 1. In order to increase the spacing combination number along the height (vertical), a total of 11 layers (named 1# to 11#) are deliberate to define the spatial distribution of wind loads. The separation of two adjacent layers varies from 0.03m to 0.3m, and the largest separation is up to 1.62m, the height of each layer is shown in table 1. For each layer there were 52 pressure taps arranged as shown in Fig. 2. In order to study the effect of wind angles on the along-wind load characteristics of rectangular building, the surface pressures were measured with the wind yaw angle varying from 0° to 90°. The 0° yaw angle was defined as the wind normal to the wider side as shown in Fig. 2.
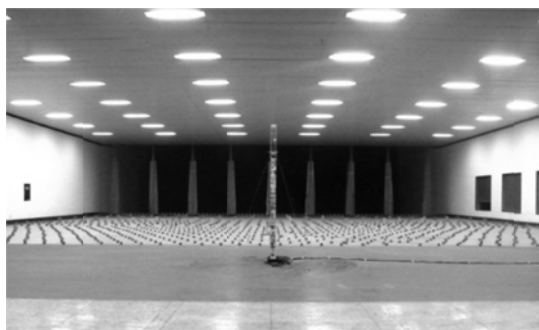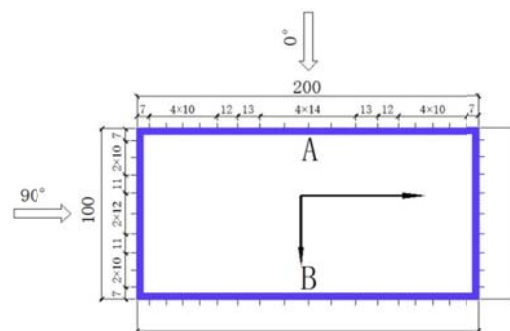

Fig. 1 Picture of the wind tunnel test

Fig. 2 Positions of the pressure taps across the rectangle section (Unit: mm)

Tab 1 The height of each layer with pressure taps (m)

Layer	1#	2#	3#	4#	5#	6#	7#	8#	9#	10#	11#
Height	0.19	0.24	0.44	0.67	0.9	1.1	1.15	1.3	1.33	1.51	1.81

The atmospheric boundary layer was simulated by traditional passive method, i.e. spires and cubes. The flow field characteristics were calibrated by Cobra Probe and the wind fluctuations in three directions were measured simultaneously. The sampling frequency of Cobra Probe and fluctuating pressures are set as 256Hz. The measured mean wind speeds (U_z) and turbulence intensities (I_u) at various heights of the test section are shown in Fig. 3, wherein z_g is the gradient wind height, U_g is the corresponding wind speed. It is shown that the profile of the mean wind speed can be fitted reasonably by the exponent model. The longitudinal turbulent spectrum at the height of 10# section is shown in Fig. 4 (n is the frequency, σ^2 is the root value). It is found that the measured results agree particularly well with von Kármán spectrum.
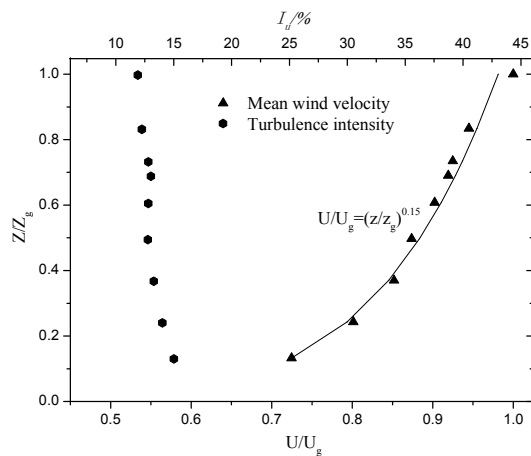

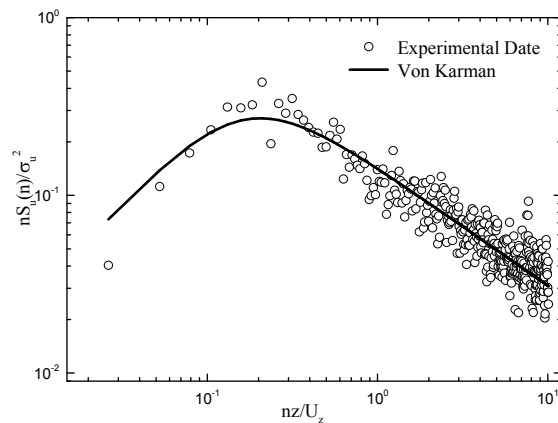Fig. 3 Average wind speed and turbulence intensity Profile

Fig. 4 Normalized wind speed spectrum

3. RESULTS AND DISCUSSIONS

3.1 Aerodynamic coefficients
The transient pressure coefficient is defined as:

$$C_{pi}(t) = \frac{P_i(t) - P_\infty}{P_0 - P_\infty},$$

(1)

In Eq. (1), $C_{pi}(t)$ is the pressure coefficient and $P_i(t)$ is the fluctuating wind pressure at the point i, P_0、P_∞ are total mean pressure at the central tap of the top level (11#) and static pressure respectively. The mean pressure coefficient $\bar{C}_{pi}$ at the point can be calculated in the entire sample interval,

$$\bar{C}_{pi} = \frac{\sum_{j=1}^{N} C_{pi}(t_j)}{N}, \tag{2}$$

In Eq. (2), *N* the number of samples, which is 30720 in this test, $C_{pi}(t_j)$ is the transient pressure coefficient at time t_j for the tap *i*. And the root-mean-square (*rms*) fluctuating $\tilde{C}_{pi}$ of wind pressure coefficients can be obtained,

$$\tilde{C}_{pi} = \sqrt{\frac{\sum_{j=1}^{N} \left(C_{pi}(t) - \bar{C}_{pi} \right)^2}{N-1}}, \tag{3}$$

By utilizing the measured results, the mean and *rms* pressure coefficients of the model with various wind angles can be obtained by Eq. (2) and Eq. (3) and makes it possible to study the wind pressure distribution on the high-rise building concerned. Traditionally, the most adverse wind direction is when the oncoming wind is normal to the wider side of the building, i.e. wind angle 0°. Fig. 5 shows the distribution of mean and *rms* pressure coefficients on windward side (side A) and leeward side (side B).

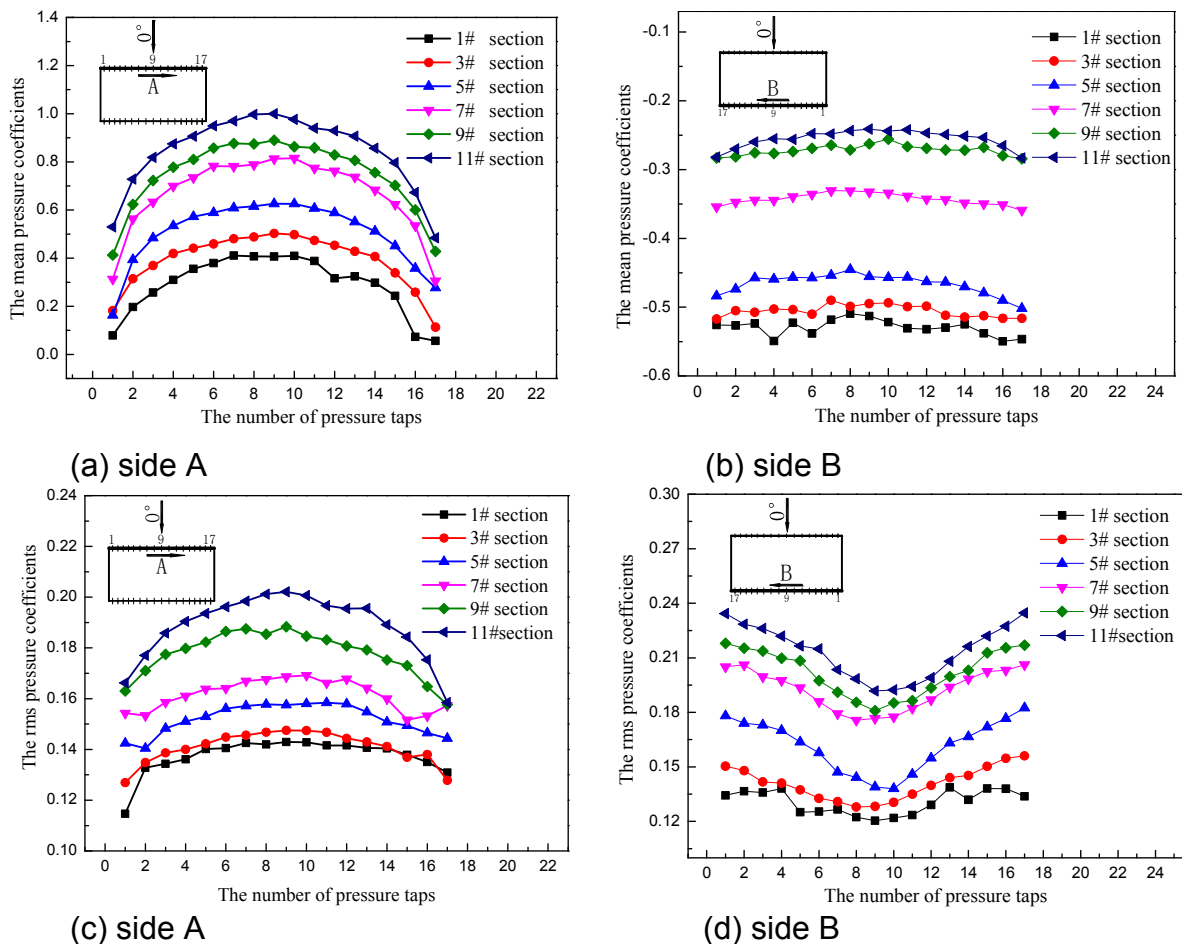(a) side A

(b) side B

(c) side A

(d) side B

Fig. 5 The mean and *rms* pressure coefficients of the rigid model under the most unfavourable wind angle

For the windward side, both the mean and fluctuating and pressure coefficients become larger with increase of the height under normal wind action (0° wind angle). The distribution mean of pressures is roughly symmetrical with respect to the axis of cross-section for each layer. A similar characteristic is observed for the fluctuating pressures, as shown in Fig. 5 (c).

The mean pressures on the leeward side take the same tendency as the ones on the windward side. Although the fluctuating pressures are also distributed symmetrically, the least rms value are found at the middle line of the leeward side, see Fig. 5 (d). It is noted that both mean and rsm pressures coefficients of the leeward side are influenced greatly by the signature turbulence induced by the body or vertex shedding. In contrast, the wind loads on windward side are determined mainly by oncoming turbulence or background flow.

3.2 power spectral characteristics

In order to describe the variations of the wind pressures along the building in frequency domain, the power spectra of fluctuating wind pressures under the 0° wind angle were analyzed. Taking section 4# (z=0.67m) and 9# (z=1.33m) as examples, the spectra of along-wind loads at windward and leeward sides were studied respectively as shown in Fig. 6. It is found that the energy contributed by the higher section is generally larger than the one of the lower section. The peak in load spectra of leeward is observed when the reduced frequency is 0.12, which is obviously induced by the vortex shedding. However, the energy induced by the vortex shedding is smaller than the ones caused by the atmospheric turbulence.
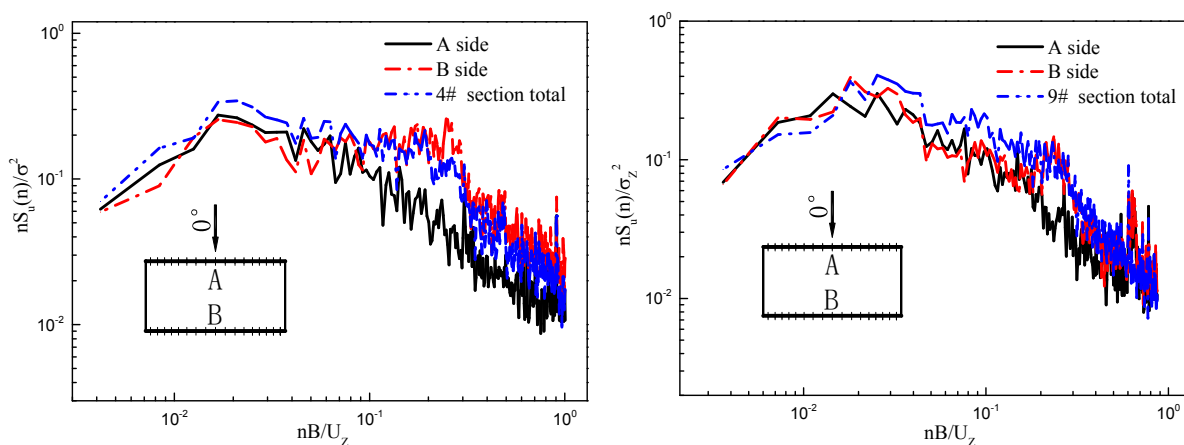

Fig. 6 Reduced power spectral densities of along-wind pressure fluctuations

3.3 coherence functions of fluctuating drag force

At present, particularly in prediction of the along-wind loads and wind-induced responses, simple exponential coherence model of gusty wind proposed by Davenport (1967) is widely used to describe the spatial distribution of the unsteady wind loads for simplicity. Krenk's study (1996) indicated that Davenport's coherence model had obvious shortcomings, and the uncertainty of the decay factor may cause serious errors.

In time domain, correlation coefficients can be used to describe the spatial correlation of fluctuating pressures between two sections along the building. Correspondingly, the coherence function is generally used in the frequency domain. Fig. 7 shows the coherence of along-wind wind load under the 0° wind angle. The correlation coefficient characteristics of fluctuating drag forces along height under wind angles 0° and 90° are shown in Fig. 8, and the correlation coefficients of fluctuating wind are also given. It can be seen that the along-wind fluctuating load are more correlated than the oncoming turbulence. The result is consistent with the conclusion of Dyrbye et al (1996). Thus, the traditional exponential coherence model for turbulence may underestimate the fluctuating wind load and risk the building. Therefore, it is necessary to propose a coherence model to describe the spatial distribution of unsteady along-wind loads.
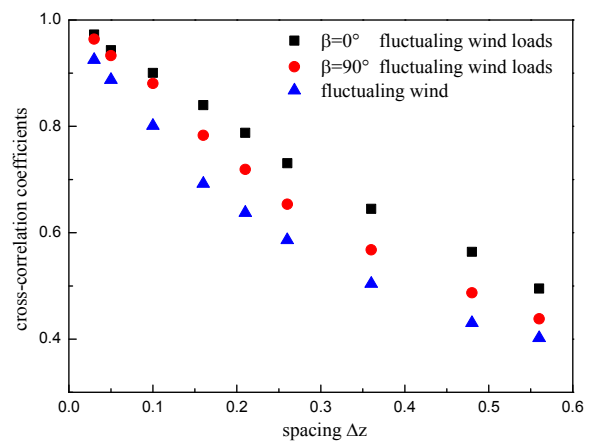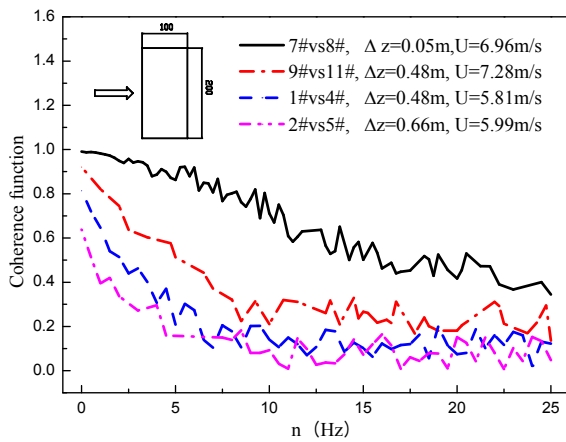

Fig. 7 Coherence function of fluctuating drag force   Fig. 8 Comparison of the correlation coefficient

Based on the measured results and inspired by the studies of Vickery (1972) & Liang (2002), the following coherence model of fluctuating drag force was proposed by taking the effect of the characteristic dimension of the building and integral length scales into consideration as:

$$Coh(n, s, \Delta z) = C_0(s) \cdot exp(-\frac{n \Delta z C_{dz}(s)}{U}), \tag{4}$$

$$s = \Delta z B^{0.1} / L_u^{1.1}, \tag{5}$$

In which, $Coh(n, s, \Delta z)$ is the coherence function of fluctuating drag force along vertical, coefficient $C_0(s)$ is varied between 0~1, which can reflect the influence of the spacing to the origin value of coherence function, C_{dz} is the decay factor, L_u is the turbulent length scales of fluctuating wind, Δz is the distance of two layers. Based on the measured results, the parameters in Eq. (4) were fitted as shown in Fig. 9:

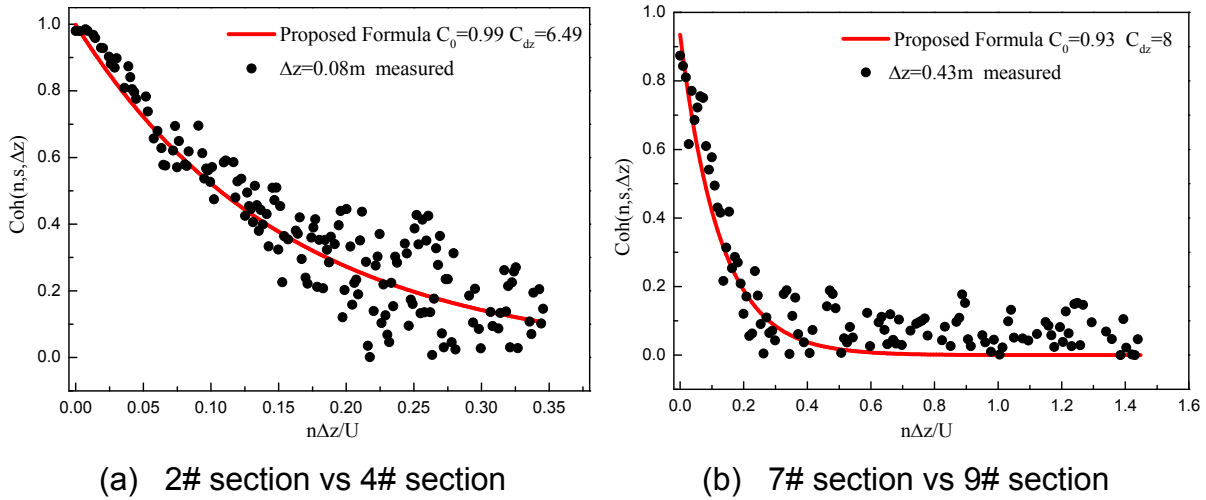(a) 2# section vs 4# section   (b) 7# section vs 9# section

Fig. 9 Comparison of coherence function between experimental date
and proposed formula

Through the fitting of the correlation function tested under the different spacing, $C_0(s)$ and $C_{dz}(s)$ expressions are obtained. The fitting results are compared with the tests and are shown in Fig.10 and Fig. 11.

$$C_0(s) = cos(s), \tag{6}$$

$$C_{dz}(s) = -5.2968s^2 + 7.1623s + 6.1054, \tag{7}$$
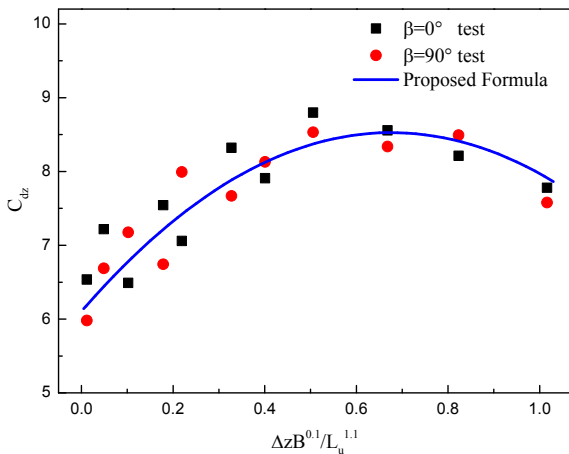

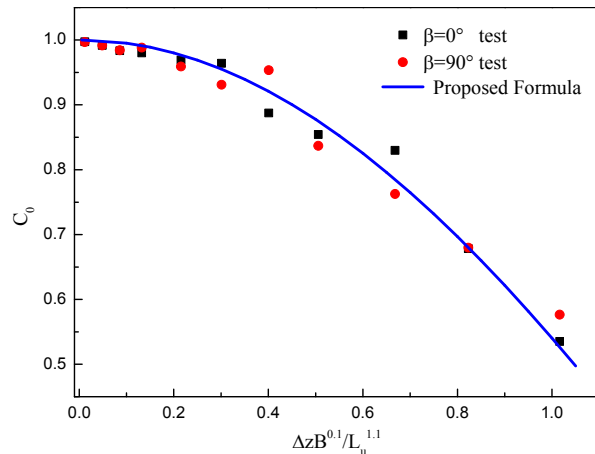Fig. 10 The decay factor $C_{dz}(s)$ Fig. 11 The factor $C_0(s)$

4. CONCLUSIONS

On the basis of extensive experimental data obtained by wind tunnel tests, the characteristic of along-wind loads on a rectangular tall building is studied in this paper. The main findings can be summarized as followings:

Under the most unfavorable wind angle, the mean and fluctuating pressure coefficient of rectangular model are increased along the height. The pressures on the each layer/section are basically symmetric, and the mean pressure coefficients of the central taps on the windward side are usually larger than others. Because of vortex shedding, the pressure fluctuations on the leeward side are apparently more severe than the windward side, and the fluctuating pressures near the corners are usually larger than the others for each layer. The energy induced by the vortex shedding is smaller than the ones caused by the atmospheric turbulence.

The along-wind fluctuating loads were more correlated than the turbulence, and the traditional coherence model of the turbulence was invalid in predicting the response of high-rise buildings. The correlation of the along-wind loads on rectangular high-rise buildings is closely related to turbulence integral length scale, vertical spacing and windward width, and increases with the increasing of turbulent flow integral length scale of turbulence, decreases with increasing frequency and the vertical distance. In addition, the coherence model propound is in good agreement with the experiment data. The application of this model may improve the accuracy of along-wind responses estimation.

REFERENCES

Davenport, A. G. (1967), "Gust loading factors." Journal of the Structural Division, **93**(3), 11-34.

Dyrbye, C., & Hansen, S. O. (1996), Wind loads on structures. John Wiley & Sons.

Gu Ming, Ye Feng, Zhang Jianguo. (2006), "Amplitude characteristics of wind loads on typical super-tall buildings." Journal of building structures, **27**(1), 24-36.

Huot, J. P., Rey, C., & Arbey, H. (1986), "Experimental analysis of the pressure field induced on a square cylinder by a turbulent flow." Journal of Fluid Mechanics, **162**, 283-298.

Kareem A. (1990), "Measurements of pressure and force fields on building models in simulated atmospheric flows." Journal of Wind Engineering and Industrial Aerodynamics, **36**, 589-599.

Krenk, S. (1996, January), "Wind field coherence and dynamic wind forces", In IUTAM symposium on advances in nonlinear stochastic mechanics (pp. 269-278). Springer Netherlands.

Liang, S., Liu, S., Li, Q. S., et al. (2002), "Mathematical model of acrosswind dynamic loads on rectangular tall buildings." Journal of Wind Engineering and Industrial Aerodynamics, **90**(12), 1757-1770.

Vickery, B. J. (1966), "Fluctuating lift and drag on a long cylinder of square cross-section in a smooth and in a turbulent stream." Journal of Fluid Mechanics, **25**(03), 481-494.

Vickery, B. J., & Kao, K. H. (1972), "Drag or along-wind response of slender structures." Journal of the Structural Division, **98**(1), 21-36.